Spontaneous *Irs1* passenger mutation linked to a gene-targeted *SerpinB2* allele

Randal J. Westrick[a,b], Karen L. Mohlke[c], Lindsey M. Korepta[d], Angela Y. Yang[b], Goujing Zhu[d], Sara L. Manning[b], Mary E. Winn[d], Kristiann M. Dougherty[d], and David Ginsburg[a,b,d,1]

[a]Life Sciences Institute and [b]Howard Hughes Medical Institute, University of Michigan, Ann Arbor, MI 48109; [c]Department of Genetics, University of North Carolina, Chapel Hill, NC 27599; and [d]Departments of Internal Medicine, Human Genetics, and Pediatrics, University of Michigan, Ann Arbor, MI 48109

Contributed by David Ginsburg, August 16, 2010 (sent for review May 6, 2010)

In characterizing mice with targeted disruption of the *SerpinB2* gene, we observed animals that were small at birth with delayed growth and decreased life expectancy. Although this phenotype cosegregated with homozygosity for the inactive *SerpinB2* allele, analysis of homozygous *SerpinB2*-deficient mice derived from two additional independent embryonic stem (ES) cell clones exhibited no growth abnormalities. Examination of additional progeny from the original *SerpinB2*-deficient line revealed recombination between the small phenotype (*smla*) and the SerpinB2 locus. The locus responsible for *smla* was mapped to a 2.78-Mb interval approximately 30 Mb proximal to *SerpinB2*, bounded by markers D1Mit382 and D1Mit216. Sequencing of *Irs1* identified a nonsense mutation at serine 57 (S57X), resulting in complete loss of IRS1 protein expression. Analysis of ES cell DNA suggests that the S57X *Irs1* mutation arose spontaneously in an ES cell subclone during cell culture. Although the *smla* phenotype is similar to previously reported *Irs1* alleles, mice exhibited decreased survival, in contrast to the enhanced longevity reported for IRS1 deficiency generated by gene targeting. This discrepancy could result from differences in strain background, unintended indirect effects of the gene targeting, or the minimal genetic interference of the S57X mutation compared with the conventionally targeted *Irs1*-KO allele. Spontaneous mutations arising during ES cell culture may be a frequent but underappreciated occurrence. When linked to a targeted allele, such mutations could lead to incorrect assignment of phenotype and may account for a subset of markedly discordant results from experiments independently targeting the same gene.

insulin receptor substrate protein | mutant strain | plasminogen activator inhibitor 2 | knockout mice | embryonic stem cell mutation

Gene targeting in embryonic stem (ES) cells has revolutionized the use of the mouse as a model organism for studying gene function in vivo, providing powerful insights into the functions of individual genes and their relationships to complex phenotypes (1). However, this methodology is technically demanding, expensive, and time-consuming, discouraging the production of multiple engineered mouse lines from independently targeted ES cell clones for confirmation of observed phenotypes. As a result, many "knockout" mouse reports are based on the analysis of animals derived from a single targeted ES cell clone. In some cases, a functional KO is obtained, despite an aberrant gene targeting event with only partial deletion or rearrangement at the targeted locus (2).

In cases in which the same locus has been independently targeted by more than one strategy, important and surprising differences have occasionally been observed. The explanations for such discrepancies include variation in genetic strain background of the gene targeted mice and structural differences in the targeted alleles (3–5). Polymorphisms in the genomic region surrounding the targeted locus between the ES cell line used for targeting and the strains used for mating, called "passenger genes," can be particularly confounding (6). Gene targeting may also unexpectedly interfere with the expression of a nearby gene, as has been observed for retained selectable marker cassettes (7–9) and probably contributes to the disparate phenotypes reported for five independent *Myf-5*/*Mrf4* targeted alleles (5, 10). It is likely that other artifacts resulting from the process of gene targeting remain to be discovered (8).

The protein product of the *SerpinB2* gene, plasminogen activator inhibitor-2 (PAI-2), is a member of the serine protease inhibitor family. Similar to PAI-1, the primary physiological function of PAI-2 is thought to be regulation of the plasminogen activators urokinase and tissue plasminogen activator in the extravascular compartment (11–13). Although PAI-2 deficiency has not yet been identified in humans, it has been proposed to play a role in additional processes including apoptosis, tumor metastasis, embryo implantation, macrophage survival, and fibrinolysis (14, 15). The high plasma levels observed during pregnancy also suggest that PAI-2 could be important for placental maintenance or during embryonic development (16). To investigate the in vivo function of PAI-2, we previously generated three *SerpinB2*-KO mouse lines derived from three independent ES cell clones identified as 15B11, 10G3, and 13B5 (17). *SerpinB2*-deficient mice derived from the 10G3 and 13B5 clones exhibited no overt phenotype, even in the context of concomitant PAI-1 deficiency (17). However, a distinct phenotype, termed *smla* because of the runted and scruffy appearance of the animals, was noted in the majority of homozygous *SerpinB2*-deficient mice obtained from the 15B11 line.

We now report the identification of the specific molecular defect responsible for the *smla* phenotype as a nonsense mutation (S57X) in a nearby gene, insulin receptor substrate 1 (*Irs1*), that appears to have originated in the ES cells used for the gene targeting.

Results

***smla* Phenotype Associated with *SerpinB2* Deficiency.** To generate *SerpinB2*-deficient mice, three targeted ES cell clones (15B11, 10G3, and 13B5) were injected into C57BL/6J blastocysts (17). Six chimeric males obtained from clone 15B11 were used to generate mice heterozygous for *SerpinB2,* and 13 F_1 heterozygous matings were initiated. Analysis of F_2 progeny alive at weaning (3 wk of age) revealed a divergence from the expected Mendelian ratios, with a trend toward decreased numbers of $SerpinB2^{15B11-/-}$ pups ($P \approx 0.051$) that reached significance when analyzing only female offspring ($P < 0.01$; Table 1). As evident in Fig. 1*A*, $SerpinB2^{15B11-/-}$ mice also exhibited significantly decreased lifespan ($P < 0.05$), with loss of $SerpinB2^{15B11-/-}$ beginning shortly after weaning. As seen in Fig. 1*B*, adult $SerpinB2^{15B11-/-}$ mice are noticeably smaller than their WT and heterozygous littermates. Normalized weights of F_2 progeny

Author contributions: R.J.W., K.L.M., K.M.D., and D.G. designed research; R.J.W., K.L.M., L.M.K., A.Y.Y., G.Z., S.L.M., M.E.W., and K.M.D. performed research; R.J.W., K.M., L.M.K., K.M.D., and D.G. analyzed data; and R.J.W., K.L.M., K.M.D., and D.G. wrote the paper.

The authors declare no conflict of interest.

[1]To whom correspondence should be addressed. E-mail: ginsburg@umich.edu.

Table 1. Genotypic analysis of weaning age F_2 progeny (15B11 cell line)

Sex	*SerpinB2* $^{+/+}$	*SerpinB2* $^{+/-}$	*SerpinB2* $^{-/-}$	Total	*P* value
Male	53 (27.6%)	87 (45.3%)	52 (27.1%)	192	≈0.5
Female	56 (30.1%)	106 (57.0%)	24 (12.9%)	186	<0.001
Total	109 (28.8%)	193 (51.1%)	76 (20.1%)	378	≈0.05

stratified by *SerpinB2* genotype are shown in Fig. 2. Consistent with their visual appearance, the normalized weight ratios of *SerpinB2*$^{15B11-/-}$ mice are significantly lower (0.62 ± 0.22) compared with WT littermate controls (1.0 ± 0.09), whereas no significant difference was observed in the weight ratios of *SerpinB2* (15B11) heterozygotes (0.94 ± 0.18) compared with WT.

Weight data obtained from birth to 6 wk for progeny from two F_1 heterozygous matings demonstrated decreased size of the *SerpinB2*$^{-/-}$ detectable at birth and more obvious at 2 wk of age. Despite their small stature, healthy adult male and female *SerpinB2*$^{15B11-/-}$ mice were fertile. Null females were able to carry null pups to term. Postmortem examination of *smla* mice identified no significant gross or microscopic abnormalities aside from the proportionally decreased stature and muscle wasting in a subset of mice. As previously reported, the *smla* phenotype was not observed in null mice from the *SerpinB2* (10G3) and *SerpinB2* (13B5) lines (17).

***smla* Is Not a Result of Maternal Effect or Known Infectious Pathogens.** Cross-fostering experiments excluded a maternal effect as the cause of the *smla* phenotype. Sera collected from *smla* mice were found to be negative for a panel of common infectious agents (*Materials and Methods*). Complementation testing between the *SerpinB2* (15B11) and *SerpinB2*^{10G3}/*SerpinB2* (13B5) alleles failed to generate any progeny with the *smla* phenotype, excluding a vertically transmitted infection or other maternally transmitted factor(s) that depend on the *SerpinB2*-deficient genotype.

Analysis of Targeting at the *SerpinB2* Locus. *SerpinB2* (15B11) was identified as a homologous recombinant by Southern blot analysis, as previously described (17). Probes were derived from 5′ sequence located outside the targeting vector and a 3′ fragment from within the targeting vector. No second site of integration was detected (17). A *neo* probe detected a fragment of the expected size from all three targeted clones, without additional fragments that would indicate another insertion site. In addition, a cDNA probe demonstrated complete deletion of all *SerpinB2* coding sequences.

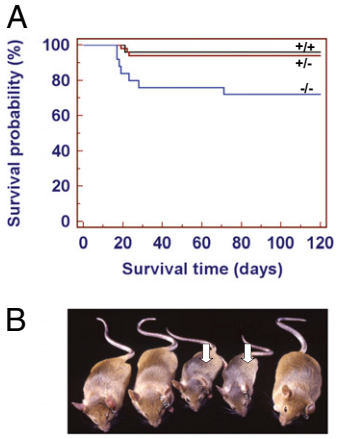

Fig. 1. Gross appearance and reduced survival of homozygous *SerpinB2*-deficient mice. (*A*) Kaplan–Meier survival analysis of WT *SerpinB2* homozygous null ($^{-/-}$) mice (*n* = 24) and heterozygous ($^{+/-}$; *n* = 51) and WT ($^{+/+}$; *n* = 25) littermates. A significant loss of homozygotes is seen, beginning at postnatal day 21, compared with WT and heterozygous animals ($P < 0.05$ and $P < 0.01$, respectively). (*B*) Five littermates from an F_1 intercross. The *smla* phenotype, indicated by the white arrows, is characterized by a grossly smaller appearance compared with WT and heterozygous littermates.

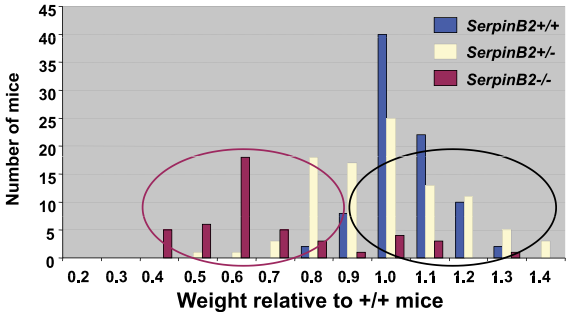

Fig. 2. Histogram of normalized weights of F2 mice from an F1 intercross of *SerpinB2*$^{+/-}$ mice. Only mice from litters containing at least one *SerpinB2* WT mouse were included (*n* = 228). With the continued generation of progeny from F_1 intercrosses of the *smla* line, occasional normally sized *SerpinB2*$^{15B11-/-}$ (red bars within the black circle) and small-sized *SerpinB2*$^{15B11+/-}$ mice (yellow bars within the red circle) were observed. These data suggest the presence of recombinants between *SerpinB2* and the locus responsible for the *smla* phenotype.

Segregation of *smla* Phenotype from *SerpinB2* Locus. With the continued generation of progeny from F_1 intercrosses of the *smla* line, normal-sized *SerpinB2*$^{15B11-/-}$ (red bars within black circle, Fig. 2) and small-sized *SerpinB2*$^{15B11+/-}$ (yellow bars within red circle, Fig. 2) were occasionally detected. Genotypes in animals with discordant phenotypes were confirmed by Southern blot analysis. The number of discordant animals was consistent with a second locus for *smla* located approximately 11 cM from the *SerpinB2* gene (Table 2).

***smla* Gene Located 26–28 Mb Centromeric to *SerpinB2*.** Analysis of mapping crosses using the CASA/RK strain revealed *smla* mice among the F_2 progeny in this mixed genetic background at the expected Mendelian frequency. Eighteen *smla* mice were chosen for genetic analysis proximal and distal to *SerpinB2* on chromosome 1. Based on the recombinant mice identified in the genetic region proximal to *SerpinB2, smla* was localized between markers *D1Mit216* and *D1Mit8*, approximately 27 Mb proximal to the *SerpinB2* locus on chromosome 1 (Fig. 3). The genotyping of 265 additional small and normally sized F_2 progeny at *D1Mit216* and *D1Mit8* and three additional markers located between *D1Mit216* and *D1Mit8* identified an additional recombinant, 8F4 (Fig. 3, bounded by the gold box), that, along with mice 8C5 and 2A8, localized *smla* to a 2.78-Mb interval between *D1Mit216* (79.8 Mb) and *D1Mit382* (82.7 Mb).

An S57X (C170A) Mutation in *Irs1* Is Responsible for *smla*. There are eight RefSeq genes within the 2.78-Mb candidate interval, including *Cul-3* (cullin-3), *Serpine2* (protease nexin 1), *Dock10*, *Irs1* (insulin receptor substrate 1), *Rhbdd1* (rhomboid domain containing protein 1), *Col4a4* (procollagen, type IV, alpha 4), *Fam124D*, and *943001J16Rik* (Fig. 3, *Bottom*). Sequence analysis of the single *Irs1* coding exon PCR-amplified from genomic DNA obtained from a *smla* mouse identified a single C-to-A transversion at nucleotide 170, resulting in a serine-to-nonsense mutation (S57X) at codon 57 (Fig. 4*A*). Genotyping of a subset of the mice with the *smla* phenotype for the C170A point mutation demonstrated complete concordance between the *smla* phenotype and homozygosity for the S57X mutation (*n* = 23).

GENETICS

Table 2. Genetically informative F_2 progeny with phenotype/genotype mismatches scored as recombinants in (*smla*/CASA/Rk) F_1 intercross progeny

Sex	*SerpinB2* $^{+/-}$	*SerpinB2* $^{-/-}$	Approximate recombinant meioses	Approximate recombinance frequency
Male	39 Normal	28 *smla*	—	—
	7 *smla*	4 Normal	11/110	0.1
Female	55 Normal	17 Normal	—	—
	1 *smla*	12 *smla*	13/114	0.11
Total	102	61	24/224	0.11

Progeny were categorized as "normal" or "*smla*" for *SerpinB2* $^{+/-}$ and $^{-/-}$ genotypes (mice with normalized weight ratios lower than 0.7 were considered *smla*, as described in *Materials and Methods*). *SerpinB2*$^{+/-}$ *smla* animals are presumably homozygous for *smla*, suggesting that a recombination has occurred on one allele between *SerpinB2* and the *smla* locus. Similarly, normal-sized *SerpinB2*$^{-/-}$ mice have presumably recombined on at least one allele between *SerpinB2* and the *smla* locus. Two recombinant meioses are possible for each *SerpinB2*$^{-/-}$ and one for each *SerpinB2* $^{+/-}$ mouse.

The S57X mutation was absent from the two other *SerpinB2* targeted null lines, as well as from WT C57BL/6J and 129S1/SvIMJ mice.

S57X *smla* Mutation Results in Loss of *Irs1* Protein Expression. The truncating S57X mutation is predicted to lead to the complete absence of IRS1 protein (Fig. 4*B*). Western blot analysis of quadriceps muscle tissue total cell extract demonstrated the expected approximate 145-kDa protein in tissue from WT and heterozygous S57X mice, with no detectable protein in tissue from mice homozygous for the S57X mutation (Fig. 4*C*).

***smla* Phenotype Is Independent of *SerpinB2* Genotype.** To exclude a contribution of *SerpinB2* deficiency to the *smla* phenotype, mice recombinant between *SerpinB2* and the S57X mutation were crossed to generate mice homozygous for *Irs1* S57X and WT at *SerpinB2*. No obvious difference in phenotype was observed among *Irs1* S57X homozygous littermates with respect to *SerpinB2* genotype.

Increased Lethality of *Irs1* Deficiency on C57BL/6J Strain Background. As detailed earlier, the *Irs1* S57X homozygous mice on a mixed 129/C57BL/6J genetic background demonstrate decreased long-term survival and runting. With further backcrossing (N3–N4 generation) into the C57BL/6J background, a marked increase in lethality was observed, with less than 2% of *Irs1* S57X homozygotes surviving to 2 wk of age (Table 3, line 1). An outcross of *Irs1* S57X heterozygotes to the 129S1/SvIMJ strain followed by F_1 intercross resulted in improved survival at 2 wk, with approximately 25% of the F_2 weanlings observed to be S57X homozygotes (Table 3, line 2).

Discussion

We previously reported the analysis of *SerpinB2*-deficient mice generated by gene targeting (17). Two independently targeted ES lines revealed no discernable abnormalities in growth, survival, development, wound healing, or macrophage recruitment (17). However, a third independent *SerpinB2*-deficient line exhibited a distinct runted phenotype, which we designated *smla*. Recombination between the *SerpinB2*-null allele and the *smla* phenotype was observed and exploited to map *smla* to a 2.78-Mb nonrecombinant interval on chromosome 1, 27 Mb proximal to

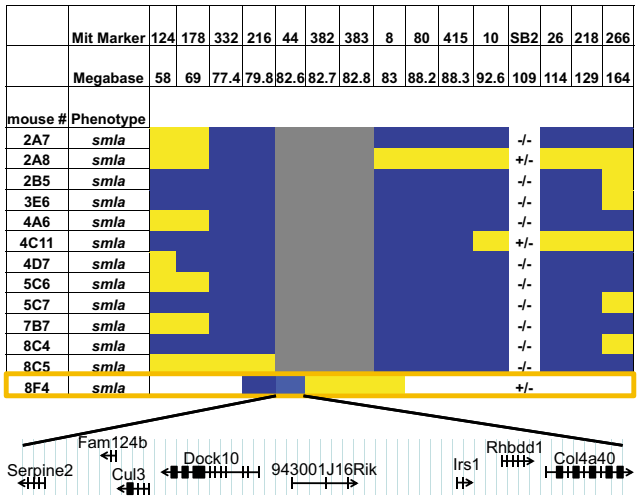

Fig. 3. Genetic map of the *smla* region on distal mouse chromosome 1. Blue boxes indicate the inheritance of two *M. musculus* alleles. Yellow boxes correspond to inheritance of one *Mus castaneus* and one *M. musculus* allele. The initial phase of mapping localized the candidate interval between markers *D1Mit216* and *D1Mit8*, shown in light gray. Recombinant 8F4, highlighted by the gold box, narrowed the right side of the interval to *D1Mit382*. Shown at the bottom is a schematic of the eight RefSeq genes contained within the minimal genetic interval. SB2, *SerpinB2*.

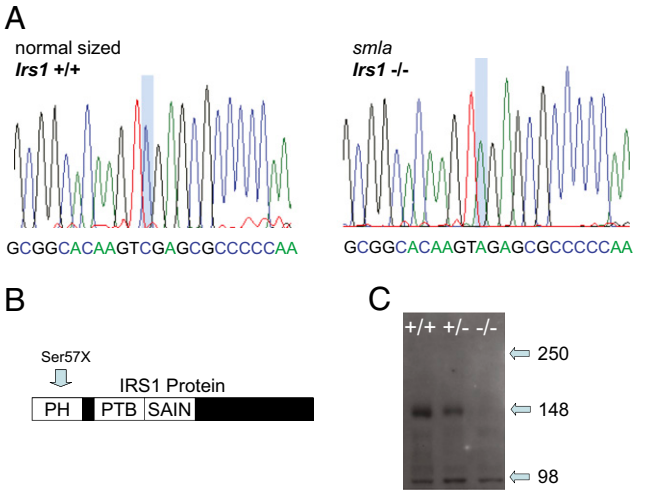

Fig. 4. Sequencing and Western blotting of *Irs1* from *smla* mice. (*A*) *Irs1* sequence tracings in the vicinity of nucleotide 170. Light blue shading highlights the presence of a "C" in the WT (*Irs1*$^{+/+}$) and an "A" in the homozygous deficient (*Irs1*$^{-/-}$) DNA sequence. This mutation results in Ser57X of IRS1. (*B*) Schematic of IRS1 protein showing that the S57X mutation disrupts all functional domains. Domains: PH, pleckstrin homology; PTB, phosphotyrosine binding, SAIN, Shc and IRS1 NPXY binding. (*C*) IRS1 Western blot of muscle tissue. There is complete absence in IRS1$^{-/-}$ and a strong signal corresponding to IRS1 protein in the IRS1$^{+/+}$ at 145 KDa. IRS1$^{+/-}$ displays an intermediate signal, consistent with one functional allele.

Table 3. Evidence of strain modifier genes affecting the survival of *Irs1* S57X homozygous mice at 2 wk of age

Gene	*Irs1*$^{+/+}$	*Irs1*$^{+/-}$	*Irs1*$^{-/-}$	Total	*P* value
C57BL/6J (N3–N4)	67 (29%)	160 (70%)	2 (0.1%)	229	$<1.4 \times 10^{-16}$
C57/129 F2	7 (15%)	27 (59%)	12 (26%)	46	0.29*

*Not significant.

SerpinB2. DNA sequence analysis of *Irs1*, a candidate gene within this nonrecombinant interval, identified a S57X nonsense mutation that truncates the protein at amino acid 57, disrupting all identified functional domains of *Irs1*. Western blot analysis of muscle tissue from S57X homozygotes revealed no reactivity compared with tissue from heterozygous and WT mice. IRS1 is a 1,231-amino acid intracellular adaptor molecule first identified as a downstream mediator of insulin receptor signaling, but also linked to several other signal transduction pathways essential for cell growth and proliferation (18, 19). Previously reported gene targeted *Irs1*-deficient mice (20–22) share a postnatal growth defect, with birth weights at 40% to 60% compared with heterozygous or WT littermates. However, in contrast to our data, no significant embryonic or postnatal lethality was observed. In addition, Selman et al. recently reported that C57BL/6 congenic *Irs1*-deficient female mice display increased longevity compared with heterozygote and WT controls (23). These results contrast with our observation of early lethality of homozygous *Irs1* S57X mice N3/N4 on the C57BL/6J background (compared with normal survival at 2 wk on a mixed C57BL/6J-129S1Sv/IMJ background).

There are several possible explanations for this discrepancy in phenotype. The *Irs1*-null allele reported here results from a single point mutation, with no other associated genomic alterations. In contrast, the previously reported null alleles contain an insertion 2.6 kb 3′ to the translation initiation start site or a deletion of −77 to +179 (21, 22). These changes in genomic structure could conceivably interfere with the expression of a nearby gene, as has been previously reported for gene targeted alleles at the granzyme B and β globin loci (7, 9), and the *Myf-5*/*Mrf4* genes (5, 10).

Mouse genetic background has a critical effect on many phenotypes (24), with strain-specific modifiers and genetic interactions previously reported in the insulin receptor pathway (20, 25, 26). Mice heterozygous for both insulin receptor (*Insr*) and *Irs1* mutations exhibit dramatically different phenotypes on the 129Sv, C57BL/6, and DBA/2 genetic backgrounds, with C57BL/6 mice displaying marked hyperglycemia and hyperinsulinemia (27). These or similar strain modifiers could contribute to the differences in survival observed for the *Irs1* S57X congenic mice on different backgrounds (Table 3), as well as with previously reported gene targeted *Irs1* mutants.

Even established inbred mouse strains maintained in isolation from one another may effectively become substrains separated from each other by hundreds of generations (28). In addition, Watkins-Chow et al. recently discovered an intrastrain copy number variant of the insulin degrading enzyme (*Ide*) present in Hardy-Weinberg equilibrium in the inbred C57BL/6J mouse population at Jackson Laboratories (29). It is possible that this or other subtle variations within C57BL/6J could contribute to discordant survival observed in the current and previous reports. Finally, differential contributions from retained 129Sv sequences within the KO congenic intervals also cannot be excluded.

A spontaneous *Irs1* mutation in an inbred C3.SW-H2b/SnJ mouse strain was also recently reported (30). Mice homozygous deficient for this mutation exhibit hyperinsulinemia, are small in stature, and exhibit bone abnormalities, with no reported effect on longevity (30). The normal lifespan observed in these mice may be a result of residual hypomorphic IRS1 function from the more distal truncation at amino acid 211, or of the difference in strain background (C3H/HeSnJ, except for a Swiss donor congenic fragment on chromosome 17).

The point mutation responsible for *smla* is likely to have arisen as a random point mutation in the ES cell line that produced *SerpinB2* (15B11). A remote effect directly resulting from the homologous recombination targeting procedure seems very unlikely, given the physical distance between the *SerpinB2* gene and *Irs1* (27 Mb). Extensive Southern blot analyses also detected no evidence for an aberrant recombination as the result of the gene targeting. *Smla* S57X homozygotes were observed among the progeny of all six chimeric founders from injection of the 15B11 clone. However, an additional *SerpinB2*-targeted clone also derived from the D3 ES cell line [*SerpinB2* (10G3)] did not generate mice with the *smla* phenotype. Taken together, these results suggest that the *smla* mutation either arose in the 15B11 clone shortly after targeting or that the S57X mutation is present in a subclone within the D3 cell line.

Although ES cell lines are generally propagated for a limited number of passages, new mutations would be expected to arise randomly during each cell division in cell culture during the gene targeting process. ES cells may also be hypersensitive to DNA damage, readily undergoing apoptosis or differentiation to remove the damaged cells from the totipotent pool (31, 32). As ES cells have been demonstrated to have enhanced mutation repair mechanisms for certain classes of mutations, such as double strand break repair, the observed mutations surviving propagation would be expected to be enriched for other classes, such as point mutations, and further selected for those that have either no deleterious or even positive growth effects on cultured ES cells (31, 32).

Although not previously reported to our knowledge, spontaneous point mutations are likely to be a common event in gene targeting experiments. Previous calculations based on human disease mutation data estimated the rate of nonsense and other clear loss-of-function mutations as approximately 3.4×10^{-6} per locus per generation (33), in excellent agreement with recent direct whole genome sequencing analysis of a family quartet (34). Assuming that one human generation corresponds to approximately 35 cell divisions yields a loss-of-function mutation rate of approximately 1×10^{-7} per locus per cell division. This number is also consistent with directly measured mutation rates at the *Aprt* and *Hprt* loci in murine ES cells (31, 35). The *SerpinB2* (15B11) allele was targeted in D3 ES cells (17) at approximately 30 cell culture passages from the isolation of the original ES cell to establish the D3 line. An estimated additional 20 passages were required for cell line maintenance and the gene targeting procedure. The assumption of approximately three cell doublings per passage yields a total of approximately 150 cell divisions, which predicts the accumulation of approximately 1.5×10^{-5} inactivating mutations per locus (or approximately 0.3 inactivating mutations per genome). This number may not fully account for missense and regulatory mutations and is thus potentially a significant underestimate. The majority of these mutations would be unlinked to the targeted locus, and thus likely to be lost during breeding to establish the line. However, a linked mutation could confound analysis, particularly of early-generation animals. Similar effects have been documented for strain-specific passenger genes (6), resulting from transgenesis or gene targeting in one mouse genetic background, subsequently backcrossed into a second strain. Selection for the targeted or transgenic allele results in retention of varying lengths of flanking DNA from the original strain, generally in the range of 10 to 30 Mb and potentially containing hundreds of genetic variants, even between highly inbred WT and transgenic littermates (6).

With the mutation frequencies estimated earlier, more than 0.6% of gene-targeted alleles would be expected to carry

a functionally significant spontaneous mutation within 30 Mb of the targeted gene. Such a mutation would be coinherited with the targeted allele, along with other strain-specific genetic differences within the same interval, potentially leading to misinterpretation of the association of phenotype with the targeted genotype, particularly if the conclusions are based on a single clone (6, 36).

Although conflicting KO phenotypes resulting from strain-specific modifier genes or differences in the anatomy of the targeting constructs have been previously documented, the impact of a new spontaneous mutation in a passenger gene should be added to the list of potential confounding genomic effects that must be taken into account for all gene targeting experiments. Although this report documents a unique spontaneous point mutation in a passenger gene, the "Fierce" phenotype observed in *Zfa*-KO mice was previously shown to be caused by a 44-kb ES cell deletion removing the *Nr2e1* gene (located approximately 10 Mb from the *Zfa* gene) (37). These two reports suggest that such spontaneous mutations may more frequently complicate gene targeting experiments than previously suspected. This is an important issue to consider in approaches to saturate the mouse genome with a library of KO alleles, particularly if only a single clone per gene is produced and/or analyzed (38). Taken together, these observations suggest that the analysis of an unexpected gene targeted phenotype should be confirmed by examination of mice derived from at least two independent ES clones.

Materials and Methods

Generation of *SerpinB2* Deficient *smla* and Normal Mouse Lines. The generation of *SerpinB2*-deficient mice was previously reported (17). A total of three independent *SerpinB2*-deficient lines were generated, two [*SerpinB2* (15B11) and *SerpinB2* (13B5)] from the 129Sv D3 cell line and one [*SerpinB2* (10G3)] from cell line CJ7 (39). Clone 15B11 from the D3 cell line was used to generate six chimeric male founder mice, which were then mated to (C57BL/6J × DBA/2J) F_1 females. B6D2 F1 mice (stock no. 100006, http://jaxmice.jax.org/strain/100006.html; Jackson Laboratory) were used for mating to the original chimeras to increase numbers of offspring. The resulting pups, which we designated F_1, were then interbred to generate progeny, which we designated as F_2. DNA prepared from tail biopsies was genotyped at the *SerpinB2* locus as previously described (17). *SerpinB2* (15B11) mice from each of the six founder lines exhibited the distinctive *smla* phenotype and were subjected to further genetic and phenotypic analysis. The *SerpinB2* (13B5) and *SerpinB2* (10G3) lines were analyzed as previously reported (17). The 10G3 line (stock no. 007234, http://jaxmice.jax.org/strain/007234.html; Jackson Laboratory) has been deposited at Jackson Laboratory and has been distributed to other investigators. All subsequent studies and reports from other groups (14, 15, 40–42) were confined to the 10G3 line. All animal care and experimental procedures complied with the Principles of Laboratory and Animal Care established by the National Society for Medical Research and were approved by the University of Michigan Committee on Use and Care of Animals.

Initial Phenotypic Analysis of *smla SerpinB2* (15B11) Deficient Mice. A total of 280 F_2 progeny of the initial F_1 intercross were used for weight analyses. Pups were weighed at weaning. To reduce the effect on weight of litter size, age at weaning, and maternal care, weights were normalized to the mean weight of *SerpinB2* WT mice within the same litter (n = 228; litters lacking *SerpinB2* WT mice were not included in this analysis). To analyze relative growth, 11 mice from two litters were weighed every 2 to 3 d from birth through 6 wk of age. Before tagging, mice were distinguished by colored nontoxic marker. Kaplan–Meier analysis was performed based on survival data from 100 mice. Sera collected from *SerpinB2*-deficient mice of the initial intercross were tested at Charles River Laboratories for the following common infectious agents: SEN, PVM, MHV, MVM, GD-VII, REO-3, MPUL, MPV, EDIM, LCMV, MAD, ECTRO, K, POLY, MTLV, MCMV, HANT, ECUN, and CARB. The effect of maternal care was evaluated by fostering pups to WT mothers (28). Autopsies were performed on one normal-sized and two *smla* 3-mo-old F_2 mice.

DNA Analysis for Aberrant Targeting. DNA was prepared as previously described (17) from ES cells of the three targeted *SerpinB2*-deficient lines as well as control nontargeted ES cells. DNA was also prepared from mice generated from the three *SerpinB2*-deficient clones. Probes included a 1-kb ScaI/HindIII fragment of the *SerpinB2* gene located 5′ to the targeting vector (probe A) and an XbaI/EcoRI fragment located within the 3′ arm of the targeting construct (probe B) as previously described (17). A *SerpinB2* cDNA probe was generated as a 1.7-kb PstI-ClaI fragment, and the neo probe consisted of a 0.5-kb PCR-amplified fragment, generated with primers described previously (17). Standard Southern blot analysis was performed on DNA digested with BglI for analysis with probe A or ScaI for analysis with probes B, *SerpinB2* cDNA or *neo*. Further Southern blot analysis was performed with probe B on mouse DNA digested with ApaI, NheI, or StuI.

Positional Cloning of *smla*. For genetic mapping, an intersubspecific outcross was performed between an inbred strain of *Mus musculus castaneus* (CASA/Rk) and three *SerpinB2*-deficient *smla* mice on a mixed *Mus musculus* background (129S1/SvIMJ, C57BL/6J and DBA/2J). The (*smla* × CASA/Rk) F_1 mice were intercrossed to produce 283 F_2 generation progeny. At weaning, pups were euthanized and weighed, and tail biopsy specimens were collected. Weights of pups were normalized to the weight of WT pups in the same litter, as described earlier. For the initial stage of mapping, *smla* mice were defined as those with normalized weight ratios lower than 0.7. Mating pairs were progeny tested to select those in which both parents carried the *smla* allele. To exclude mice with runted phenocopies, only mating pairs producing two or more *smla* pups that were nonrecombinant across the candidate interval were used for subsequent mapping. Initially, 18 *smla* mice were genotyped for 13 markers from mouse chromosome 1 (*D1Mit124, 178, 332, 216, 8, 415, 10, 26, 218, 263, 498, 199, 266*). Genotyping was performed as previously described (43), and the 129S1/SvIMJ, C57BL/6J and DBA/2J *M. musculus* alleles were considered as one equivalent class for mapping purposes, as compared with the *M. musculus castaneus* allele.

For further analysis, 265 additional F_2 mice from a (CASA/Rk × *smla*) F_1 intercross were studied. After localization of *smla* between markers *D1Mit216* and *D1Mit8*, both small and normal-sized F_2 progeny were genotyped at these two markers. Mice recombinant between *D1Mit216* and *D1Mit8* were genotyped at *D1Mit44, 382*, and *383* (three additional markers located between *D1Mit216* and *D1Mit8*).

***Irs1* Sequence Analysis.** A series of primer pairs were designed using the primer3 program (http://biotools.umassmed.edu/bioapps/primer3_www.cgi) to generate overlapping PCR amplicons approximately 500 bp in length that span the entire coding region of *Irs1* (44). PCR was performed on DNA isolated from a mouse with the *SerpinB2* (15B11) *smla* phenotype. PCR amplicons were purified using the Qiaquick PCR gel extraction kit (Qiagen), sequenced, and assembled into a contig using DNAStar (Lasergene), then compared with the publicly available *M. musculus* sequence (GenBank accession no. NM_010570).

Genotyping the *Irs1* Point Mutant. The *Irs1* C170A point mutation was genotyped by analysis of a 190-bp PCR product generated with the following primers: 5′, CTT CTC AGA CGT GCG CAA GG; 3′, GTT GAT GTT GAA ACA GCT CTC. The C170A mutation abolishes a Taq1 restriction site (TCGA to TAGA) at position 143 of the PCR product.

Western Blotting. The quadriceps muscles of WT, heterozygous, and IRS1 Ser57X homozygous mutants were excised, snap-frozen, and homogenized. Homogenates were then fractionated on a 4% to 12% SDS/PAGE gel and probed with a rabbit anti-rat polyclonal antibody (45, 46). This antibody was generated against a peptide corresponding to the sequence of the COOH-terminal 14 aa of rat IRS1 (Millipore). The Western blot was run with the SeeBlue Plus2 prestained standard (Invitrogen).

Influence of Disparate Genetic Contexts on Survival of *Irs1*-Deficient Mice. Heterozygous *Irs1* C170A point mutants were backcrossed to C57BL/6J for six generations and segregated away from the *SerpinB2*-deficient allele. An intercross of the N6 backcrossed heterozygous mice was analyzed for surviving mice of each genotype at weaning. N6-backcrossed mice were then outcrossed to 129S1/SvIMJ and the F_1 progeny intercrossed to produce the F_2 generation. Survival of each possible genotype of the F_2 mice was assessed at 2 wk.

Statistics. Data from mouse crosses were statistically analyzed using the χ^2 test. Weight differences were evaluated by t test. Survival was analyzed by Kaplan–Meier method, with significance determined by the log-rank test.

ACKNOWLEDGMENTS. The authors acknowledge the University of Michigan transgenic core for technical assistance in generating the *SerpinB2*-null mice by gene targeting. We thank Thom Saunders and Alexey Kondrashov for valuable discussions regarding mutation rates in ES cells. This study was supported by National Institutes of Health Grants R01 HL039693 and P01 HL057346. R.J.W. was supported in part by an American Heart Association predoctoral fellowship. D.G. is a Howard Hughes Medical Institute Investigator.

1. Mak TW (2007) Gene targeting in embryonic stem cells scores a knockout in Stockholm. *Cell* 131:1027–1031.
2. Kobayashi S, et al. (1998) DNA sequence motifs are associated with aberrant homologous recombination in the mouse macrophage migration inhibitory factor (Mif) locus. *Gene* 215:85–92.
3. Grubb BR, Gabriel SE (1997) Intestinal physiology and pathology in gene-targeted mouse models of cystic fibrosis. *Am J Physiol* 273:G258–G266.
4. Lahvis GP, Bradfield CA (1998) Ahr null alleles: Distinctive or different? *Biochem Pharmacol* 56:781–787.
5. Olson EN, Arnold HH, Rigby PW, Wold BJ (1996) Know your neighbors: Three phenotypes in null mutants of the myogenic bHLH gene MRF4. *Cell* 85:1–4.
6. Lusis AJ, Yu J, Wang SS (2007) The problem of passenger genes in transgenic mice. *Arterioscler Thromb Vasc Biol* 27:2100–2103.
7. Pham CT, MacIvor DM, Hug BA, Heusel JW, Ley TJ (1996) Long-range disruption of gene expression by a selectable marker cassette. *Proc Natl Acad Sci USA* 93: 13090–13095.
8. Scacheri PC, et al. (2001) Bidirectional transcriptional activity of PGK-neomycin and unexpected embryonic lethality in heterozygote chimeric knockout mice. *Genesis* 30: 259–263.
9. Fiering S, et al. (1995) Targeted deletion of 5′HS2 of the murine beta-globin LCR reveals that it is not essential for proper regulation of the beta-globin locus. *Genes Dev* 9:2203–2213.
10. Kaul A, Köster M, Neuhaus H, Braun T (2000) Myf-5 revisited: loss of early myotome formation does not lead to a rib phenotype in homozygous Myf-5 mutant mice. *Cell* 102:17–19.
11. Kruithof EK, Baker MS, Bunn CL (1995) Biological and clinical aspects of plasminogen activator inhibitor type 2. *Blood* 86:4007–4024.
12. Medcalf RL, Stasinopoulos SJ (2005) The undecided serpin. The ins and outs of plasminogen activator inhibitor type 2. *FEBS J* 272:4858–4867.
13. Lobov S, Croucher DR, Saunders DN, Ranson M (2008) Plasminogen activator inhibitor type 2 inhibits cell surface associated tissue plasminogen activator in vitro: Potential receptor interactions. *Thromb Haemost* 100:319–329.
14. Tonnetti L, et al. (2008) SerpinB2 protection of retinoblastoma protein from calpain enhances tumor cell survival. *Cancer Res* 68:5648–5657.
15. Park JM, et al. (2005) Signaling pathways and genes that inhibit pathogen-induced macrophage apoptosis—CREB and NF-kappaB as key regulators. *Immunity* 23: 319–329.
16. Kruithof EK, et al. (1987) Fibrinolysis in pregnancy: A study of plasminogen activator inhibitors. *Blood* 69:460–466.
17. Dougherty KM, et al. (1999) The plasminogen activator inhibitor-2 gene is not required for normal murine development or survival. *Proc Natl Acad Sci USA* 96: 686–691.
18. Saltiel AR, Pessin JE (2002) Insulin signaling pathways in time and space. *Trends Cell Biol* 12:65–71.
19. Thirone AC, Huang C, Klip A (2006) Tissue-specific roles of IRS proteins in insulin signaling and glucose transport. *Trends Endocrinol Metab* 17:72–78.
20. Kido Y, et al. (2000) Tissue-specific insulin resistance in mice with mutations in the insulin receptor, IRS-1, and IRS-2. *J Clin Invest* 105:199–205.
21. Tamemoto H, et al. (1994) Insulin resistance and growth retardation in mice lacking insulin receptor substrate-1. *Nature* 372:182–186.
22. Araki E, et al. (1994) Alternative pathway of insulin signalling in mice with targeted disruption of the IRS-1 gene. *Nature* 372:186–190.
23. Selman C, et al. (2008) Evidence for lifespan extension and delayed age-related biomarkers in insulin receptor substrate 1 null mice. *FASEB J* 22:807–818.
24. Westrick RJ, Winn ME, Eitzman DT (2007) Murine models of vascular thrombosis (Eitzman series). *Arterioscler Thromb Vasc Biol* 27:2079–2093.
25. Withers DJ, et al. (1999) Irs-2 coordinates Igf-1 receptor-mediated beta-cell development and peripheral insulin signalling. *Nat Genet* 23:32–40.
26. Kido Y, Philippe N, Schäffer AA, Accili D (2000) Genetic modifiers of the insulin resistance phenotype in mice. *Diabetes* 49:589–596.
27. Kulkarni RN, et al. (2003) Impact of genetic background on development of hyperinsulinemia and diabetes in insulin receptor/insulin receptor substrate-1 double heterozygous mice. *Diabetes* 52:1528–1534.
28. Silver L (1995) *Mouse Genetics, Concepts and Applications* (Oxford Univ Press, New York).
29. Watkins-Chow DE, Pavan WJ (2008) Genomic copy number and expression variation within the C57BL/6J inbred mouse strain. *Genome Res* 18:60–66.
30. DeMambro VE, et al. (2010) A novel spontaneous mutation of Irs1 in mice results in hyperinsulinemia, reduced growth, low bone mass and impaired adipogenesis. *J Endocrinol* 204:241–253.
31. Tichy ED, Stambrook PJ (2008) DNA repair in murine embryonic stem cells and differentiated cells. *Exp Cell Res* 314:1929–1936.
32. Van Sloun PP, et al. (1999) The role of nucleotide excision repair in protecting embryonic stem cells from genotoxic effects of UV-induced DNA damage. *Nucleic Acids Res* 27:3276–3282.
33. Kondrashov AS (2003) Direct estimates of human per nucleotide mutation rates at 20 loci causing Mendelian diseases. *Hum Mutat* 21:12–27.
34. Roach JC, et al. (2010) Analysis of genetic inheritance in a family quartet by whole-genome sequencing. *Science* 328:636–639.
35. Cervantes RB, Stringer JR, Shao C, Tischfield JA, Stambrook PJ (2002) Embryonic stem cells and somatic cells differ in mutation frequency and type. *Proc Natl Acad Sci USA* 99:3586–3590.
36. Eisener-Dorman AF, Lawrence DA, Bolivar VJ (2008) Cautionary insights on knockout mouse studies: The gene or not the gene? *Brain Behav Immun* 23:318–324.
37. Kumar RA, et al. (2004) Unexpected embryonic stem (ES) cell mutations represent a concern in gene targeting: Lessons from "fierce" mice. *Genesis* 38:51–57.
38. Zambrowicz BP, Friedrich GA (1998) Comprehensive mammalian genetics: History and future prospects of gene trapping in the mouse. *Int J Dev Biol* 42:1025–1036.
39. Swiatek PJ, Gridley T (1993) Perinatal lethality and defects in hindbrain development in mice homozygous for a targeted mutation of the zinc finger gene Krox20. *Genes Dev* 7:2071–2084.
40. Losick VP, Isberg RR (2006) NF-kappaB translocation prevents host cell death after low-dose challenge by Legionella pneumophila. *J Exp Med* 203:2177–2189.
41. Lijnen HR, Frederix L, Scroyen I (2007) Deficiency of plasminogen activator inhibitor-2 impairs nutritionally induced murine adipose tissue development. *J Thromb Haemost* 5:2259–2265.
42. Darnell GA, et al. (2006) SerpinB2 is an inducible host factor involved in enhancing HIV-1 transcription and replication. *J Biol Chem* 281:31348–31358.
43. Mohlke KL, et al. (1996) A novel modifier gene for plasma von Willebrand factor level maps to distal mouse chromosome 11. *Proc Natl Acad Sci USA* 93:15352–15357.
44. Rozen S, Skaletsky H (2000) Primer3 on the WWW for general users and for biologist programmers. *Methods Mol Biol* 132:365–386.
45. Ueki K, et al. (2000) Restored insulin-sensitivity in IRS-1-deficient mice treated by adenovirus-mediated gene therapy. *J Clin Invest* 105:1437–1445.
46. Taniguchi CM, Ueki K, Kahn R (2005) Complementary roles of IRS-1 and IRS-2 in the hepatic regulation of metabolism. *J Clin Invest* 115:718–727.